SLAC-PUB-798
September 1970
(EXPI)

MAGNETIC SPECTROMETERS*

W. K. H. Panofsky

Stanford Linear Accelerator Center
Stanford University, Stanford, California 94305

(Review talk presented at the High Energy Physics
Instrumentation Conf., Sept. 8-12, 1970, Dubna, USSR)

*Work supported by the U.S. Atomic Energy Commission.

I. INTRODUCTION

In this paper I am to talk on recent progress in magnetic spectrometers designed for use at high particle energies.

We are faced with the problem how to define a high energy magnetic spectrometer. In a certain sense almost all the devices which are the subject of this conference might be considered to be magnetic spectrometers if they involve magnets at all. If I were to describe all recent developments where a magnet is used to determine a particle energy, most of the topics of this conference would be included. I will restrict this discussion only to those devices especially designed for analysis of particles emanating from a target where emphasis is placed on measuring the production angles and momenta. This means I will emphasize those devices where resolution and identification of the process under study is achieved primarily through production kinematics and not through time coincidence or decay mechanism.

Spectrometers naturally fall into two general classes: (1) "Small" aperture spectrometers, usually, but not always, used as "single arm" detectors of particles emanating from a target; (2) "Large" aperture spectrometers dedicated to the analysis of multi-body events.

Spectrometers are complex systems; Fig. 1 shows the components of a generalized spectrometer arrangement: particles pass through a magneto-optical system and their path is traced by track detectors and other counters. A number of these counters feed a "trigger logic" which initiates a decision whether the data relating to a track are to be stored for read-out by a computer and eventual data storage and analysis. In this paper I will restrict myself primarily to reviewing the magnetic elements only since discussion of detectors and data handling and analysis is being covered by other authors at this conference.

II. SMALL APERTURE, SINGLE ARM SPECTROMETERS

A. General

Single arm spectrometers can be broadly categorized into those where detection takes place after magnetic analysis and those where detection and particle identification and magnetic analysis are intimately intertwined. Spectrometers can further be subdivided into focusing and nonfocusing spectrometers. In a focusing spectrometer the momentum or the production angle of the particle can be identified in a focal plane without detailed ray tracing of each particle through the entire magnetic system. Again there is no sharp division between a focusing and a nonfocusing spectrometer because, even if the spectrometer generates its primary information in the focal plane, some coincidence planes are generally added which permit some rudimentary ray tracing to derive auxiliary quantitites which might be valuable in controlling aberrations.

B. Focusing Spectrometers with Particle Detection and Identification after Magnetic Analysis

Several papers have been published discussing in general terms design criteria for high resolution focusing spectrometers. Some of these emphasize the formal aspects of beam transport theory such as the work of Brown[1] and others, while other papers[2] are dedicated to general discussions more specifically pointed to experiments.

There are a large number of parameters which influence the design of a spectrometer; however, the most important factors are the resolution and the solid angle acceptance of the system. However, the accessible intensity may be also controlled by the target length which can be seen by the spectrometer, in particular since the primary target is generally liquid hydrogen.

The focusing action of a spectrometer can either be point-to-point focusing or line-to-point focusing. In the vertical plane point-to-point focusing generally assures maximum acceptance, while in the horizontal plane the situation is more complex. If maximum target length is to be used, and if the required resolution in production angle is a small fraction of the total angular acceptance, then line-to-point focusing is advantageous, since the focal point in the horizontal plane gives a measure of the production angle. The problem is that if focusing in the horizontal plane is to give a measure of production angle, then momentum measurement has to be achieved by vertical dispersion. This means that the mechanical problem in designing such spectrometers becomes large as the energy is increased.

The spectrometers at SLAC are possibly the largest examples of spectrometers which will be built in which momentum dispersion is vertical and angular information is generated by horizontal focusing. These spectrometers have been described previously in the literature, both in summary papers[3,4] and in the publications describing the experimental work undertaken with these instruments. I will therefore only give a brief outline.

Three spectrometers having maximum momenta of 1.6 GeV/c, 8 GeV/c and 20 GeV/c, respectively, are rotating about a common pivot; Fig. 2 shows a photograph of the installation. Each of these incorporates vertical dispersion in momentum and horizontal line-to-point focusing. The spectrometers cover angular regions matched to their maximum accepted momenta. Table 1 shows the first order focal properties for each of the spectrometers. The optical properties have been verified by calibration in the primary SLAC electron beam.

The momentum resolution of these instruments is controlled primarily by the relative magnitudes of momentum dispersion and vertical magnification;

thus the vertical spot size controls the attainable resolution. Table I summarizes these basic quantities. The second and higher order aberrations control the resolution in production angle and also ultimately control momentum resolution if the source size is small. The second order effects are discussed separately for each spectrometer.

The 1.6 GeV spectrometer[4] consists of a single magnet only, as shown in Fig. 3. It is basically a weak-focusing device using a 90° vertical bend and using wedge focusing at the exit and entrance pole faces. The pole faces are designed to make the production angle and momentum focal planes coincident in space. Second order corrections are made in three places along the magnet by introduction of pole curvature which results in making the focal planes normal to the central ray. Table II compares the measured and theoretical values of some of the first and second order coefficients of the magnet. The attainable resolution is $\pm$ 0.08%. If the instrument is used for the study of two-body reactions then for each value of center-of-mass energy there is a unique kinematic relation between production angle and secondary particle momentum. Over the range of acceptance of the instrument this kinematic relationship would define a straight line in the focal plane in which production angle and momentum are dispersed at right angles. It is therefore possible to rotate a simple hodoscope into alignment along the appropriate kinematic curve. Thus this type of spectrometer does not require computer decoding of signals in successive hodoscope planes and therefore data can be taken at exceedingly high rates.

Unfortunately this simple system becomes infeasible economically if momenta above the 2 GeV range are to be analyzed. The 8 GeV spectrometer is composed of three separate quadrupoles which provide the required focusing

and two rectangular bending magnets of uniform field for dispersion. Figure 4 shows the complete spectrometer assembly, including the shielding surrounding the detector. Table III shows the comparison between the theoretical and measured first order matrix elements as observed. Due to the fact that the fringing fields of neighboring magnets affect one another, or possibly due to minor perturbations resulting from steel in the support structure, the effective length of the quadrupoles is not known precisely from measurements on the separate magnets. Therefore the table shows parameters under operating conditions adjusted such that the principal first order coefficients are matched to theory.

It will be noted that the emerging ray of the 8 GeV spectrometer is not horizontal, and therefore the detector arrangement has to slope upwards, giving rise to complex mechanical support problems for the detector assembly. Also the focal planes for momentum focusing and production angle focusing are not in the same place and the momentum focal plane is not perpendicular to the direction of the emerging particles. From general transport theory pertaining to these devices it can be seen that the required sextupole corrections to erect the focal plane would be excessive, and would introduce other aberrations. Therefore separate hodoscopes are needed for these two focal planes; these initially are scintillation hodoscopes but will eventually be replaced by proportional wire chambers.

The problem of the particles not emerging horizontally from the spectrometer has been obviated in a somewhat complex manner in the design of the SLAC 20 GeV/c spectrometer. Its dispersive elements consist of four bending magnets, the first two of which bend the beam upwards and the second two bend the beam downward again. It can be shown by general transport theory that the

momentum dispersion of a spectrometer is proportional to the magnetic flux linked between the central ray and a ray starting at a finite angle at the source and returning to a focus. Since the two magnetic bends are in opposite directions the basic point-to-point focusing orbit in the vertical plane will have to have a cross-over midway between the two bends; thereby the effective flux linkage between the central orbit and the focusing orbit has the same sign in both halves of the orbit. Figure 5 shows a diagram of the assembled system and Table IV gives the table of the measured transfer coefficients which can be used to compute the resolution. Some of the second order coefficients, in particular those increasing with vertical angle, are quite large and therefore for highest resolution it is occasionally necessary to restrict the vertical aperture of the instrument. While the additional cross-over is necessitated in this design in order to avoid a vertically rising emerging beam, such an additional cross-over results in a disadvantage as far as second order aberrations are concerned. The addition of sextupole lenses is required for this instrument in order to erect the focal plane from its initial value between 1^{o} and 2^{o} to the central beam axis to an acceptable value.

Spectrometers dispersing momentum vertically and production angle horizontally, and which at the same time are rotatable in angle, require considerable mechanical support structures and electromechanical devices for tracking detector supports and shields with the magnets. Therefore most spectrometers constructed more recently use horizontal momentum dispersion and resolve the production angle by hodoscopes incorporated in the design; the spectrometers at DESY are of this type. Lower energy vertical dispersion spectrometers have been constructed at CEA and NINA and incorporate the basic optical elements similar to the 8 GeV/c instrument described above. A NINA installation uses

two small aperture spectrometers in coincidence with one of them permitting adjustment in vertical production angle.

C. Focusing Spectrometers as Mixed Systems with Detection and Focusing Action Mixed

As one proceeds to higher energies the question of particle identification becomes progressively more serious. In the spectrometers described in the previous section particle identification is achieved by adding such devices as Cerenkov counters, total absorption shower counters, muon range telescopes, etc., after the final hodoscopes in the focal planes. Clearly, particle identification or rejection of unwanted particles could be improved if detection devices could be introduced early in the system. Depending on duty cycle and incident fluxes, this is generally possible, and depending on the nature of the experiment, it is even possible to use detectors in the primary beam or ahead of the aperture of the spectrometers. Moreover, pole-face screening detectors have occasionally been used in order to gate out events where particles scatter off pole faces and other apertures. As we will discuss later in connection with wide aperture spectrometers, a mixed system frequently involves competition between the multiple scattering effect of the intermediate detectors and the magneto-optic resolving power of the spectrometer. The reintroduction of proportional chamber multiple channel devices has greatly alleviated this problem.

In "mixed" focusing spectrometer systems designed for highest energy, point-to-point focusing in both planes is generally adopted. Orthogonal separation of momentum dispersion and production angle dispersion appears impractical at the highest energies, since the expense associated with the solution of the mechanical problems involving a vertical bend becomes prohibitive.

If momentum dispersion is carried out in a horizontal plane, then production angle can only be "tagged" by hodoscopes following or preceding the momentum focus. Also, at higher energies the dimensions of the entire instrument scale up, while the target length is controlled by other factors. Therefore, in a point-to-point focusing scheme a sufficiently large target length can generally be kept in view, even if line-to-point focusing is not used.

For the sake of illustration I will discuss the simplest form of a mixed focusing spectrometer, namely, a symmetrical instrument in which we have a sequence of focusing lenses, a bending element again followed by focusing lenses. The bending element is broken into two halves such that the focused orbits move along parallel trajectories both vertically and horizontally in the space between the bending magnets. Figure 6 shows such an arrangement schematically. It is at this point where particle discriminators such as "DISC" Cerenkov counters can be introduced. An important point of consideration, therefore, is the angular excursion from ideal parallelism which the rays would have in the space occupied by these counters. In general the deviation from parallelism will be proportional to the initial angular aperture in the planes in question, and will also depend on the momentum band accepted by the instrument. Therefore, the use of a Cerenkov counter may require a limit on the solid angle acceptance; however, in practice the maximum momentum band is apt to be restricted by other factors. Typically, a momentum spread of ± 1% is acceptable and so are spot sizes of 1 mm and angular acceptances of 1 mr, if the DISC counter is to separate pions from kaons at 200 GeV/c.

There is a direct relation between the attainable momentum resolution $\Delta p/p$ of a point-to-point focusing spectrometer and the geometrical parameters shown in Fig. 6. This relation is

$$\frac{\Delta p}{p} = \frac{4(x_0\theta_0)\, B\rho}{\phi} \qquad (1)$$

where ($B\rho$) is the magnetic rigidity. This formula implies that spot size should be minimized while the flux linkage ϕ should be maximized. Calculations using this formula, applied to the basic symmetric configuration shown in Fig. 7, have been carried out by K. Pretzl[2] as a function of the length L of each quadrupole element. The results are summarized in Fig. 8. Shown are the vertical and horizontal angular acceptances, the accepted solid angle, and the "full width at half maximum" resolution for a 200 GeV/c spectrometer assumed to disperse in the horizontal plane with a bending field integral of 250 kG-meter. The resolution improves linearly with increase of this field integral.

This discussion assumes that resolution is controlled entirely by the entering phase space of the particles and the focusing properties of the spectrometer. This situation can be drastically improved by the introduction of intermediate wire planes which effectivcly code elements of the phase space. If such hodoscopes are used the beam size is no longer controlling but either the spacial resolution of the hodoscopes or second order aberrations become the dominant factor.

If the incident flux permits this, a proportional wire chamber (W_1) might be introduced near the target, while two chambers (W_2 and W_3) might be introduced in the detector space, one of them (W_2) being near or at the (tilted) focal plane. (Fig. 9) If W_1 and W_2 are thus placed at conjugate foci, the effect of multiple scattering is eliminated. This is a principal advantage of using a focusing over a nonfocusing spectrometer even in a "mixed" design of hodoscopes and magnets. In principle only second order aberration will control the resolution in such a design if the wire planes have sufficient resolution; detailed calculations show that the introduction of wire planes can improve the resolution over that shown in Fig. 7 by about a factor of 10 for a given bending integral and solid angle for a 200 GeV/c spectrometer.

I am including a table of parameters (Table V) of a design for a 200 GeV instrument for such a symmetrical spectrometer, which has been proposed to the National Accelerator Laboratory.

An interesting feature of spectrometers of this type is that one could construct them in two halves: If the first half were constructed only, then a set of decoding planes composed of wire chambers could be placed into what would become the future mid-region. Ray tracing through such decoding planes gives information of comparable resolution but of course less particle selection than a final spectrometer with a DISC counter in the mid-plane.

Several versions of a "point-to-parallel beam" instrument have been studied;[6] the nominal parameters of such a half-spectrometer are given in Table VI. Such a spectrometer could be built as a "first step" leading to the more powerful "point-to-point" instrument described above.

It is a matter of interest whether a focusing spectrometer offers an advantage at all over a nonfocusing spectrometer using ray tracing by two sets of wire chamber planes ahead and after the bend. We assume, of course, that the leading wire chambers will not have an excessive counting rate to make such an arrangement impossible. For instance Lach[7] and collaborators have proposed for use at the National Accelerator Laboratory a single arm, nonfocusing spectrometer using projected extremely high resolution (.05 mm) wire planes ahead of its aperture. The parameters of this instrument are shown in Table VII; a very compact design suitable for use in low particle flux results.

The general question of the merit of focusing vs nonfocusing designs has been studied by K. Pretzl[2] of NAL using two competing designs at 200 GeV using either focusing or nonfocusing designs, but otherwise having the same resolution and solid angle acceptance. The analysis concluded that a focusing

design, in addition to its other advantages, is more economical. Although a focusing spectrometer requires separate quadrupoles the required physical size of the main bending elements is much reduced in the focusing design. In addition a focusing spectrometer has numerous other advantages: Detector sizes are reduced, a DISC counter can be used, and performance is less sensitive to multiple scattering in the wire planes. Table VIII lists the comparative design parameters for a 200 GeV/c instrument of 16 μ-steradian solid angle acceptance and $\pm$ 0.05% resolution. Clearly the focusing spectrometer yields a more economic and satisfactory design.

In general I would conclude that a focusing spectrometer remains an essential and powerful tool at the highest accelerator energies.

III. WIDE APERTURE SPECTROMETERS

A. General

Large aperture spectrometers are designed to analyze more than one particle at a time. The target can either be internal or external to the magnet and the spectrometer may be operated in coincidence with other systems.

The largest controlling costs of a spectrometer system are becoming (a) the cost of the magnet, and (b) the cost of computation. We will show that the magnet cost will scale with the spatial resolution of the detector used. Therefore the future cost of powerful wide aperture spectrometer systems will critically depend on the development of such devices as liquid ionization chambers, high resolution proportional chambers, scintillation chambers scanned with high resolution electronic image devices, etc. These developments are discussed elsewhere in this conference; in this discussion I will assume that attainable spatial resolutions are fixed generally between $\pm$ 0.2 mm to $\pm$ 0.4 mm. However

some pending developments in proportional chamber techniques extend hope of reducing these figures.

The cost of computation is looming as the controlling factor in the adaptation of large aperture magnetic spectrometers to the analysis of high energy multibody events. It is therefore essential that computer consideration be incorporated into the initial design. Observation of well over 10^7 multibody events/year is an objective of several currently planned installations and the question must be answered conclusively how the fitting and analysis of these events can be accomplished at a computation cost much less than that pertaining to bubble chamber analysis. An ingredient to such cost reduction is careful magnet design; for instruments using targets external to the magnetic field, orbit reconstruction programs can be simplified if the magnet provides for (a) high field uniformity (b) perpendicular entry of particles into the field, and (c) a short fringing field.

B. Size of Magnet

The size of a wide aperture magnet is controlled by the permissible momentum error which in turn is determined by the spatial resolution Δx of the detectors used. Geometrical considerations show that the momentum uncertainty Δp is given by the relation

$$\Delta p \ \alpha \ \frac{\Delta x}{B} \left(\frac{p}{L}\right)^2 \qquad (2)$$

This scaling equation assumes that there is a fixed number of chamber planes in the magnet; since the number of planes can increase linearly with L, the scaling of Δp with L becomes $L^{-5/2}$ rather than L^{-2} if the space is fully used by increasing the number of measurement points linearly with L. The factor of proportionality in the scaling equation depends on the number, character and location of detector planes used, and, as we will discuss later, also will depend on whether additional detector planes can be located outside the magnet.

In high energy applications it is generally necessary to hold the momentum uncertainty to less than 0.1 GeV/c so that the missing mass uncertainty shall be less than the mass of the neutral pion. Numerically this means, for instance, that a 15 kG magnet with aperture 2 meters in width and 1.25 meters in height would be required if the detector resolution is assumed to be ± 0.4 mm and if wire planes were used inside the magnet only. This calculation neglects multiple scattering in the wire planes, which we will consider shortly.

It is clear from the basic resolution equation that the transverse dimensions of the magnet scale directly with the transverse momentum of the decay products studied. On the other hand the length of the magnet is proportional to the incident momentum; in the example above the required length of the magnet would be about 4 meters for an incident momentum of 40 GeV/c.

For a practical design multiple scattering in the detector planes and the gas in the path of the beam are important considerations. This means that in practice one would like to match the effect of multiple scattering and of the spatial resolution of the detectors on the over-all resolution. A second consideration affecting the size of the required magnet deals with the efficiency with which the decay products of the reaction to be studied are accepted. If the target is external to the magnet then the finite solid angle of acceptance makes it generally necessary to conduct Monte Carlo calculations to estimate detection efficiency and biases introduced into decay distributions. Figure 10 shows the results of some efficiency calculations carried out by Luste and Leith[8] for the reactions $\pi^- + p \longrightarrow A^- + p$ and $\pi^- + p \longrightarrow \rho^o + p$ for an incident pion energy of 16 GeV, computed for three apertures of a magnet operating at 16 kG. Figure 11 shows the results of similar calculation for the reaction $\pi^- + p \longrightarrow \rho^o + p$ for the detection efficiency as a function of the decay angles of the ρ^o into two

pions. In these calculations the target is assumed to be at a distance of 2.5 m from the entrance face of the magnet. It is further assumed that detectors downstream of the magnet will not control the efficiencies.

C. Multiple Scattering

The accuracy of momentum determination is given by a combination of the measurement error Δp_{meas} and multiple scattering errors Δp_{ms}

$$\text{i.e.,} \quad \left(\frac{\Delta p}{p}\right)^2 = \left(\frac{\Delta p}{p}\right)^2_{meas} + \left(\frac{\Delta p}{p}\right)^2_{ms} \tag{3}$$

The appropriate expression for $(\Delta p)_{ms}$ has been discussed extensively;[9,10] an approximate expression is:

$$\left(\frac{\Delta p}{p}\right)_{ms} = \frac{.5}{LB} (X)^{1/2} \tag{4}$$

where X is the thickness of matter measured in radiation lengths (assumed uniform) as traversed by the particles and units otherwise are kG and meters.

D. Total Measurement Accuracy

The combined error can be computed for specific configurations. Figure 12 shows a plot of the combined error computed for 1 detection plane per 3 cm, with each plane equivalent to 1/2800 radiation length thick. Curves are plotted for particles of momenta 20 GeV/c and 100 GeV/c.

The curves of Fig. 12 show that a "match" between the two sources of error is attained at a magnet length of approximately 3 m for 20 GeV/c particles and 6 m for 100 GeV/c particles. At the optimum the combined accuracy is about 7 % per kilogauss at 20 GeV/c and 5% per kilogauss at 100 GeV/c. At 15 kG field this would give a momentum error of ± 0.33 GeV at 100 GeV/c. Therefore at the higher energy an accuracy in momentum measurement corresponding to one pion mass becomes difficult.

In order to improve the attainable precision (which, as we have seen becomes marginal at highest momenta) Osborne[11] has analyzed geometries with wire chambers external to the magnet in order to obtain additional leverage; he predicts a considerable improvement in accuracy of momentum measurement (about a factor of 5); more detailed numerical calculation makes this factor appear optimistic.

E. Practical Developments

A very large number of wire spark chamber, optical spark chamber, scintillation counter hodoscopes, and proportional chamber combinations with large magnets have been constructed or are being developed in many parts of the world which deserve the name "wide aperture spectrometers." With apologies to the constructors of these devices I will mention only a very small number of specific arrangements which have singular features.

The largest wide aperture routine spectrometer operation has been evolving under the direction of Lindenbaum and collaborators.[12] His present configuration consists of two magnets, each 1.2 meters by 1.2 meters in pole face area, combined with very large high resolution magnetostrictive read-out wire planes. The arrangement can be used with a second, lower resolution, wide aperture spectrometer in order to analyze double-Vee events. The high resolution arm has attained a resolution of 0.8% momentum in tests conducted at 10 and 15 GeV/c. Figure 13 gives the experimental arrangement as planned for the latter part of 1970. Since, as discussed previously, higher incident particle momenta require a longer spectrometer but not a wider one, Lindenbaum is proposing cascading spectrometer magnets of this kind to constitute a spectrometer for particles to be analyzed for use at high energies at the National Accelerator Laboratory. Figure 14 shows the mass spectrum of neutral kaons identified via their pion decays in the spectrometer.

Another recent development is the evolution of spectrometers using internally curved proportional chambers. Such an arrangement is being installed in a magnet of 1.2 meter by 1.2 meter with a 60 cm gap at the Cornell University 10 GeV Electron Synchrotron by a group from the University of Chicago and the University of Pennsylvania. The purpose is to study the hadronic products from inelastic electron scattering on the proton. Figure 15 shows the arrangement. Several technical problems have to be solved before this arrangement can become operational; however, construction of the curved proportional chambers has made excellent progress. This type of arrangement has the obvious advantage of providing a very high geometrical efficiency for particles emerging from the target. Booth et al.[13] have proposed to the National Accelerator Laboratory to construct a magnet and curved proportional chamber arrangement along similar principles as those now under test at Cornell. They propose a magnet of 2-meter gap, 3-meter width, and 6-meter length operating at 20 kG, although other magnets may be substituted. Figure 16 shows the proposed arrangement.

A development project for a wide aperture spectrometer of many new features is being undertaken at SLAC.[14] The general layout of the system as presently envisaged is shown in Fig. 17. The spectrometer has two magnetic elements: (a) a large aperture (2.8 m × 1.8 m) analyzing magnet, and (b) a superconducting solenoid surrounding the target. The large analyzing magnet has curved pole pieces with the production target at the center of curvature. Moreover a superconducting mesh is used to "short out" the fringing flux lines; this device combined with a conventional mirror plate greatly shortens the fringing field. These two measures result in perpendicular entry angles and only momentum dependent exit angles through very short fringing fields; these facts substantially reduce

the computation time for orbit reconstruction. From current results on a 1/10 scale model the nonuniformity of the field integral has been demonstrated to be less than 2%.

The solenoid serves two purposes: (1) many of the wide angle tracks which otherwise would not enter the magnet aperture are retained; (2) the slow forward tracks which could not enter the field of the big magnet can be tracked by detectors in the solenoid. The field strength needed for this solenoid is still under study. If a field of 50 kG is used the solenoid will trap all particles of transverse momentum less than 550 MeV/c, which comprises a large majority of all products of strong interactions. The over-all acceptance of the system for the final pions in such reactions as $\pi^- + p \longrightarrow A^- + p$; $A^- \longrightarrow \rho^o + \pi^-$; $\rho^o \longrightarrow \pi^+ + \pi^-$ initiated by 16 GeV pions increases from 40% without the solenoid to 95% for the 50 kG field. Geometrical biases are correspondingly reduced. The instruments shown have reasonable performance for analysis of decay products of mass-states up to 3.5 GeV and missing mass resolution is projected to be adequate to detect the loss of neutral pions. Parameters for the system are still being optimized.

The largest wide aperture spectrometer arrangement now under construction is the well known CERN Omega project. The magnet assembly is to be completed by November 1971 and operation with the beam could start by May 1972. Figure 18 shows the current design giving the magnet and other dimensions. This wide aperture spectrometer will be installed in the slow-ejected proton beam near the ISR project at CERN. The expected performance of this general purpose installation has been well documented and will not be repeated here. Many of the general design considerations discussed above derive from studies carried out in conjunction with the Omega project.

May I conclude by again apologizing to the many authors who have legitimate claims to having made important contributions to the spectrometer art but whose work has not been mentioned. The subject of magnetic spectrometers is a large one and the boundaries limiting the field can be drawn almost anywhere.

REFERENCES

1. K. L. Brown, Report No. SLAC-75 and K. L. Brown and S. K. Howry, Report No. SLAC-91, Stanford Linear Accelerator Center (1969).
2. See e.g., K. P. Pretzl, NAL Report TM-233, Batavia, Illinois, April 1970.
3. W.K.H. Panofsky, Proceedings of the International Symposium on Electron and Photon Interactions at High Energies, Hamburg, Germany, June 8-12. (1965).
4. R. L. Anderson, D. Gustavson, R. Prepost, D. Ritson, Nucl. Instr. Methods 66, 328 (1968).
5. A. L. Read et al., NAL Proposal No. 64, Batavia, Illinois.
6. R. L. Anderson et al., NAL Proposal No. 73, Batavia, Illinois.
7. Lach et al., NAL Proposal No. 69, Batavia, Illinois.
8. G. Luste and D.W.G.S. Leith, private communication.
9. R. L. Gluckstern, Nucl. Instr. Methods 24, 381 (1963).
10. The Omega Project, Revised Edition, CERN Internal Report 68-11, May (1968).
11. L. S. Osborne, NAL 1969 Summer Study No. 86, Vol. 3, p. 267, Batavia, Illinois.
12. S. J. Lindenbaum, 'Multiparticle Magnetic Spectrometers with Electronic Digitized Detectors," 2nd Inter. Conf. on Experimental Meson Spectroscopy, Philadelphia, May 1-2, 1970, BNL-14877, Aug. 1970. Other references to this program given in this report.
13. Booth, Mo, Selove and Teng, NAL Proposal No. 33, Batavia, Illinois.
14. D.W.G.S. Leith and G. J. Luste, Report No. SLAC-PUB-754, Stanford Linear Accelerator Center, (1970).

LIST OF TABLES

TABLE I

THE SLAC SPECTROMETERS

Maximum Momentum	Solid Angle Acceptance	Momentum Dispersion (Vertical)	Vertical Magnification	Dispersion Due to Production Angle	Momentum Acceptance
1.6 GeV/c	4.1×10^{-3} ster	4.19 cm/% $\frac{\Delta p}{p}$	0.661	0.823 cm/mrad	± 5%
8 GeV/c	10^{-3} ster	2.907 cm/% $\frac{\Delta p}{p}$	0.928	4.575 cm/mrad	± 2%
20 GeV/c	10^{-4} ster	3.259 cm/% $\frac{\Delta p}{p}$	1.17	1.623 cm/mrad	± 2%

TABLE II

MEASURED AND THEORETICAL VALUES OF SOME OF THE 1st AND 2nd ORDER COEFFICIENTS OF THE 1.6 GeV/c SPECTROMETER

Coefficient	Theoretical Value	Experimental Value	Source of Measurement
$\langle y/\delta \rangle$ momentum dispersion	4.19 cm per %	4.19 $\pm$ 0.05 cm/%	Wire float
$\langle x/\theta_0 \rangle$ angular dispersion	0.823 cm per mr	0.823 $\pm$ 0.038 cm per mr	Electron beam spot survey
$\langle \phi/\phi_0 \rangle$ relation of input to output angles	1.514	1.52 $\pm$ 0.02	Wire float
$\langle y/\delta^2 \rangle$	6.07×10^{-2} cm/(%)^2	4.95 $\pm 1.0\times10^{-2}$ cm/(%)^2	Wire float
$\langle x/\theta_0\delta \rangle$	1.25×10^{-2} cm/mr · %	1.24 $\pm 10^{-2}$ cm/mr · %	Electron beam spot survey
$\langle y/\phi_0\delta \rangle$	1.03×10^{-3} cm/mr · %	≈ 0	Electron beam spot survey
$\langle y/\phi_0^2 \rangle$	2.47×10^{-4} cm/(mr)^2	$\approx 2.5\times10^{-4}$ cm/(mr)^2	Electron beam spot survey

The notation used is that given by Brown.[1]

δ is the momentum difference from the central orbit.

y is the displacement at the focal plane along the "momentum" axis.

ϕ_0 is the input angle in the momentum plane.

ϕ is the output angle in the momentum plane.

x is the displacement in the focal plane along the "angular axis."

θ_0 is the input "production" angle.

TABLE III

MEASURED VALUES (AT 8 GeV/c) AND TRANSPORT PREDICTIONS FOR 1st AND 2nd ORDER

MATRIX ELEMENTS FOR 8 GeV/c SPECTROMETER

First Order: Measured values above the Transport prediction

	x_0	θ_0	ϕ_0	δ_0	y_0
x	0.028 cm/cm 0.028*	4.575 ± 0.050 cm/mrad 4.575*	-0.019 cm/mrad 0.	0.027 cm/% 0.	-0.0021 0.00
θ	-0.194 mrad/cm -0.189	4.858 mrad/mrad 4.893	-0.020 mrad/mrad 0.	0.071 mrad/% 0.	0.0074 mrad/cm 0.00
y	-0.002 cm/cm 0.	0.007 cm/mrad 0.	-0.004 cm/mrad -0.014	-2.907 ± 0.029 cm/% -2.907*	not measured -0.928
ϕ	-0.008 mrad/cm 0.	0.027 mrad/mrad 0.	-1.077 mrad/mrad -1.090	0.094 mrad/% 0.203	-0.0041 mrad/cm -0.014

*Measured values equal Transport predictions by definition.

Second Order: (only the largest matrix elements listed)

	Measured	Predicted
$\langle x/x_0\delta \rangle$	0.0433 cm/cm · %	0.0428 cm/cm · %
$\langle x/\theta_0\delta \rangle$	-0.0104 cm/mrad · %	-0.0135 cm/mrad · %
$\langle \theta/y_0\delta \rangle$	0.0484 mrad/cm · %	0.0450 mrad/cm · %
$\langle \theta/\theta_0\delta \rangle$	-0.0236 mrad/mrad · %	-0.0282 mrad/mrad · %
$\langle y/\phi_0\delta \rangle$	0.0120 cm/mrad · %	0.0126 cm/mrad · %
$\langle \phi/\delta\delta \rangle$	-0.0486 mrad/$(\%)^2$	-0.0505 mrad/$(\%)^2$

The notation used is that given by Brown[1].
δ is the momentum difference from the central orbit.
y is the displacement at the focal plane along the "momentum," or vertical, axis.
ϕ_0 is the input angle in the momentum plane.
ϕ is the output angle in the momentum plane.
x is the displacement in the focal plane along the "angular," or horizontal, axis.
θ is the input "production" angle.

TABLE IV

MEASURED 1st AND 2nd ORDER MATRIX ELEMENTS FOR THE 20 GeV/c SPECTROMETER

First Order:	$\langle x/\theta_0 \rangle$	$= 1.623 \pm 0.016$ cm/mrad	$\langle y/\delta \rangle$	$= 3.259 \pm 0.033$ cm/%
	$\langle x/x_0 \rangle$	$= -0.023$ cm/cm	$\langle y/\phi_0 \rangle$	$= -0.015$ cm/mrad
	$\langle y/y_0 \rangle$	$= +1.17$	$\langle \phi/\phi_0 \rangle$	$= 0.804$ mrad/mrad
Second Order:	$\langle x/\theta_0^2 \rangle$	$= +9.2 \times 10^{-3}$ cm/(mrad)^2	$\langle y/\theta_0^2 \rangle$	$= -2.09 \times 10^{-2}$ cm/(mrad)^2
	$\langle x/\theta_0\delta \rangle$	$= +2.70 \times 10^{-2}$ cm/mrad · %	$\langle y/\theta_0\phi_0 \rangle$	$= -6.2 \times 10^{-3}$ cm/(mrad)^2
	$\langle x/\theta_0\phi_0 \rangle$	$= +1.47 \times 10^{-2}$ cm/(mrad)^2	$\langle y/\phi_0^2 \rangle$	$= -4.1 \times 10^{-3}$ cm/(mrad)^2
	$\langle x/\phi_0^2 \rangle$	$= +3.6 \times 10^{-3}$ cm/(mrad)^2	$\langle y/\phi_0\delta \rangle$	$= -6.3 \times 10^{-3}$ cm/mrad · %

The notation used is that given by Brown.[1]

δ is the momentum difference from the central orbit.

y is the displacement at the focal plane along the "momentum," or vertical, axis.

ϕ_0 is the input angle in the momentum plane.

ϕ is the output angle in the momentum plane.

x is the displacement in the focal plane along the "angular" or horizontal axis.

θ_0 is the input "production" angle.

TABLE V

PERFORMANCE PARAMETER OF A SINGLE ARM FOCUSING SPECTROMETER PROPOSED TO NAL[8] FOR HIGH FLUX USE

Length	Maximum Momentum	Solid Angle Acceptance	Momentum Resolution (Full Width)	Angular Accuracy (Full Width)	Maximum Input Flux at Aperture
220 m	200 GeV/c	4.5 μster.	0.03%	0.1 mrad	10^{10} particles/sec

TABLE VI

NOMINAL PARAMETERS OF POINT-TO-PARALLEL BEAM SPECTROMETERS CONSISTING OF ONE HALF OF THE ELEMENTS OF THE SPECTROMETER OF TABLE V

Length	Maximum Momentum	Solid Angle Acceptance	Resolution	Accuracy in Production Angle	Acceptable Particle Rate
55 m	200 GeV	16 μster.	~.04%	0.5 mrad	~10^{10} particles/sec
55 m	75 GeV	50 μster.	~.04%	0.5 mrad	

TABLE VII

PERFORMANCE PARAMETERS OF SINGLE ARM NONFOCUSING SPECTROMETER PROPOSED TO NAL[7] FOR LOW FLUX USE BUT CAPABLE OF HIGH RESOLUTION

0.05 mm PROPORTIONAL WIRE CHAMBER RESOLUTION ASSUMED.

Length	Maximum Momentum	Solid Angle Acceptance	Momentum Resolution (Full Width)	Angular Accuracy (Full Width)	Maximum Input Flux at Aperture
33 m	200 GeV/c	25 μster.	0.05%	0.02 mrad	$\sim 10^6$ particles/sec

TABLE VIII

COMPARISON OF FOCUSING SPECTROMETER VERSUS

NONFOCUSING SPECTROMETER

Constant in both cases:

$p = 200$ GeV/c $\quad \Delta p/p = \pm 0.05\% \quad \Delta = 16\ \mu$ster.

	Focusing Spectrometer	Nonfocusing Spectrometer
Total length	70 m	120 m
Detector	Wire proportional chamber	Wire proportional chamber
Number of detectors	3	4
Spatial resolution in detectors	± 0.5 mm	± 0.5 mm
Distance between detectors before or behind spectrometer magnets	12 m	50 m
$\Delta p/p$ limited by multiple scattering by detectors	± 0.004%	± 0.012%
Number of quadrupoles	4	0
Number of bending magnets ($B_{max} \approx 15$ kG, length 6 m each)	3	3
Magnet gap g	7.5 cm	20 cm
Magnet width W	25 cm	60 cm
DISC counters	yes	no

LIST OF FIGURES

12. Plot of the product of magnetic field and momentum resolution against magnet length. Both the resolutions due to measurement and due to multiple scattering are shown.

13. The double wide aperture spectrometer of Lindenbaum and collaborators as configured for operation late in 1970.

14. K_0 mass spectrum obtained by Lindenbaum and collaborators in a test run using the BNL wide aperture spectrometer.

15. Experimental spectrometer arrangement under test by Mo and Selove at the Cornell 10 GeV electron synchrotron.

16. Experimental spectrometer arrangement for analyzing the products of inelastic muon scattering prepared by Booth et al.[17] for use at NAL.

17. Schematic layout of the large aperture SLAC spectrometer under development. The analysis system is projected to consist of two separate field volumes, the large aperture magnet downstream and a superconducting solenoid around the target. The solenoid is 1.5 m in diameter, and 2.5 m long with the magnetic field of ~50 kG, along the beam line. A system of cylindrical, and plane, spark chambers measure the slow particles within the solenoid, while a series of conventional wire chambers in front and behind the large magnet (2.8 m × 1.8 m gap) measure the forward going particles. The chambers will range in size from (2.5 m × 1.5 m) in front, to (5 m × 4 m) behind.

18. Geometry of the CERN Omega Spectrometer as configured December 1970.

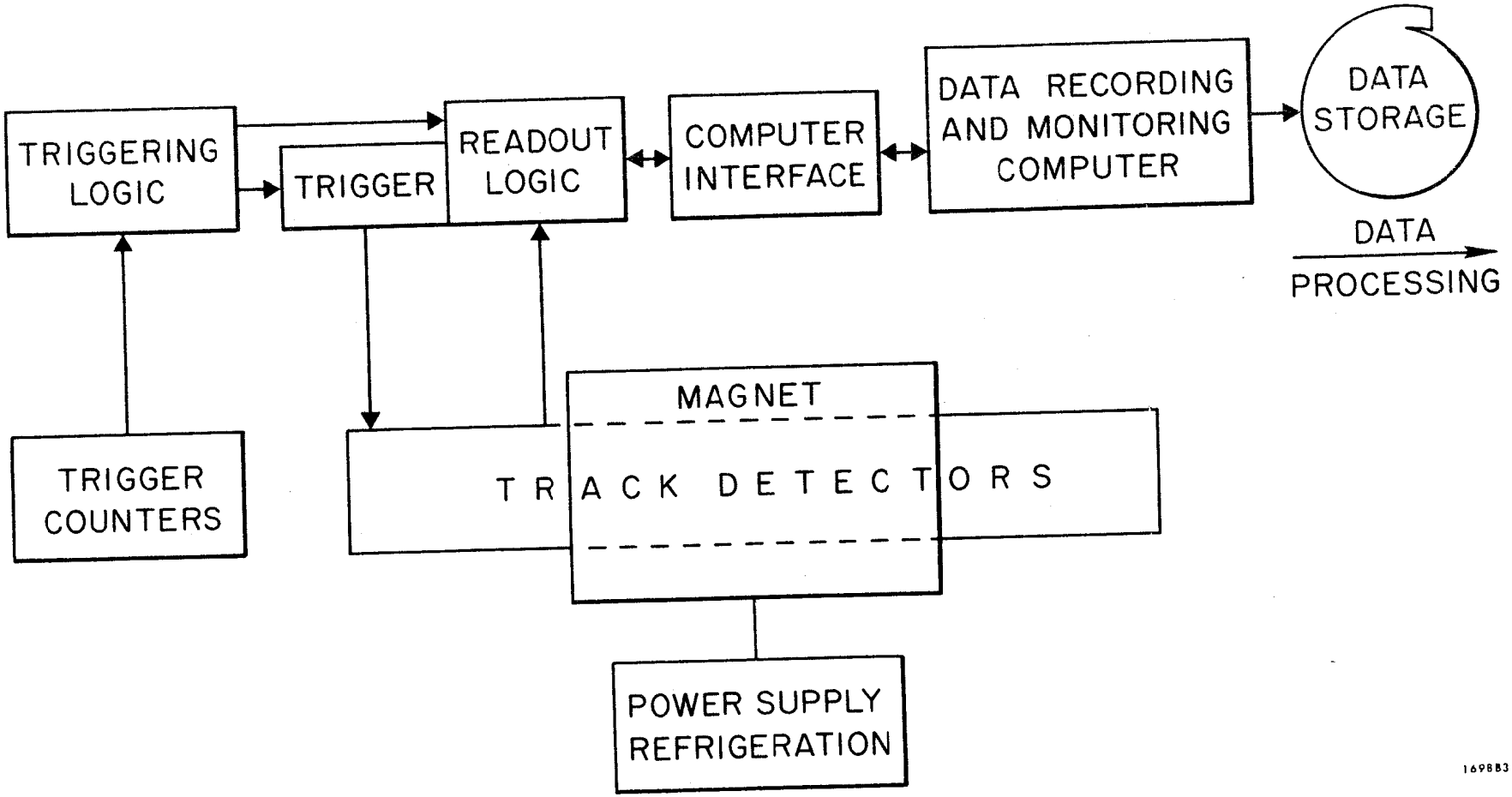
TRIGGERING LOGIC
TRIGGER
READOUT LOGIC
COMPUTER INTERFACE
DATA RECORDING AND MONITORING COMPUTER
DATA STORAGE
DATA
PROCESSING
MAGNET
TRACK DETECTORS
TRIGGER COUNTERS
POWER SUPPLY REFRIGERATION
169883

Fig. 1

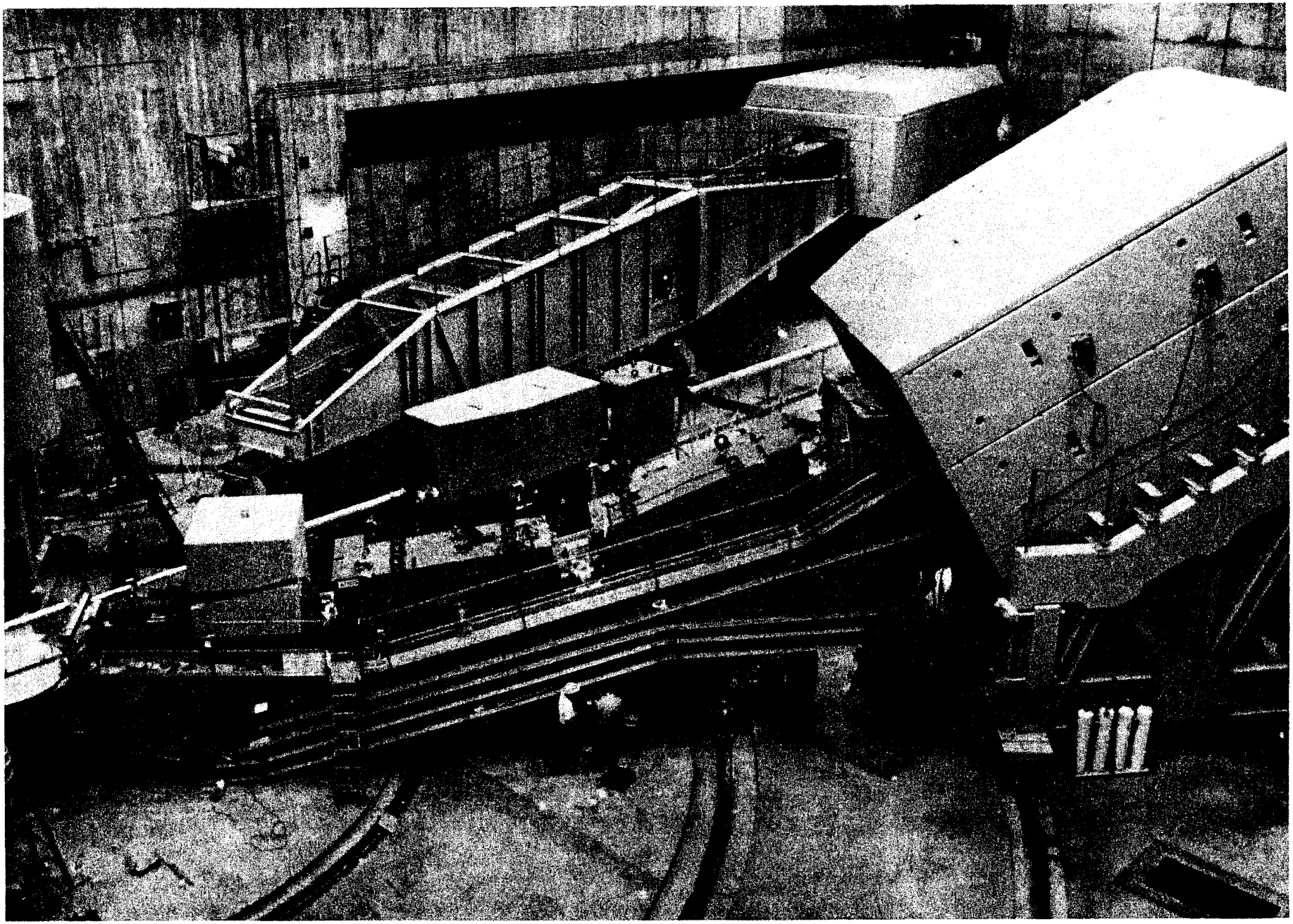

Fig. 2

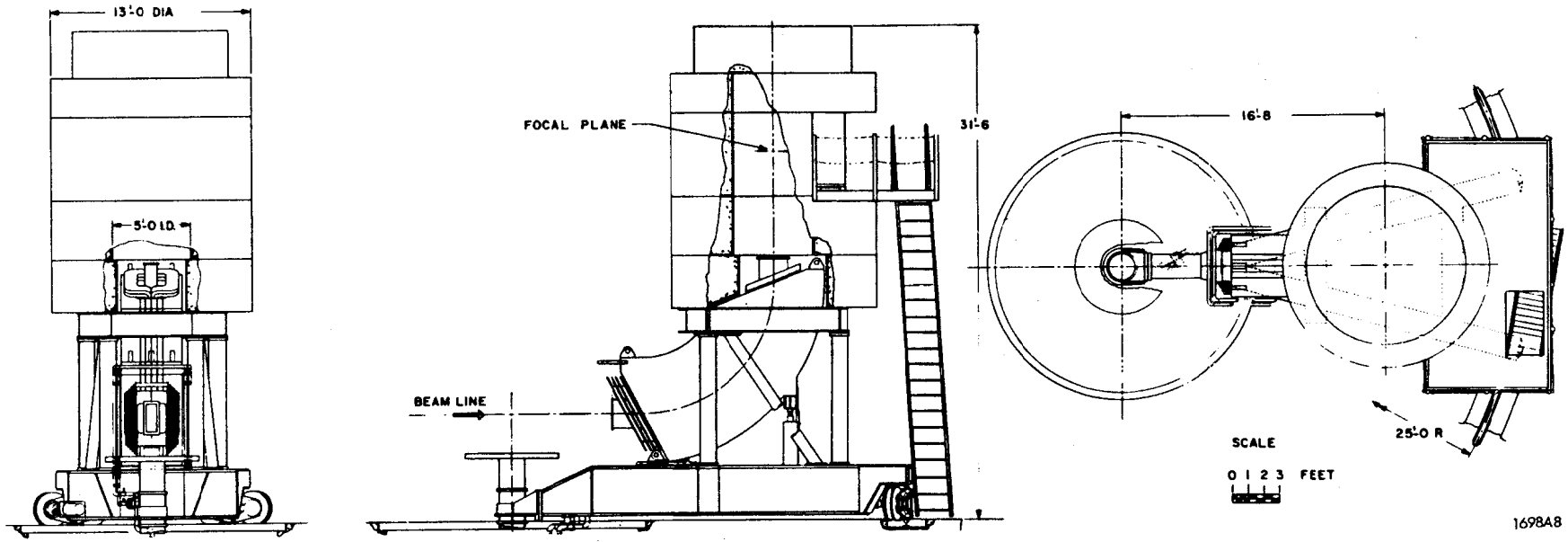
13'-0 DIA
5'-0 I.D.
FOCAL PLANE
31'-6
BEAM LINE
16'-8
25'-0 R
SCALE
0 1 2 3 FEET
169848

Fig. 3

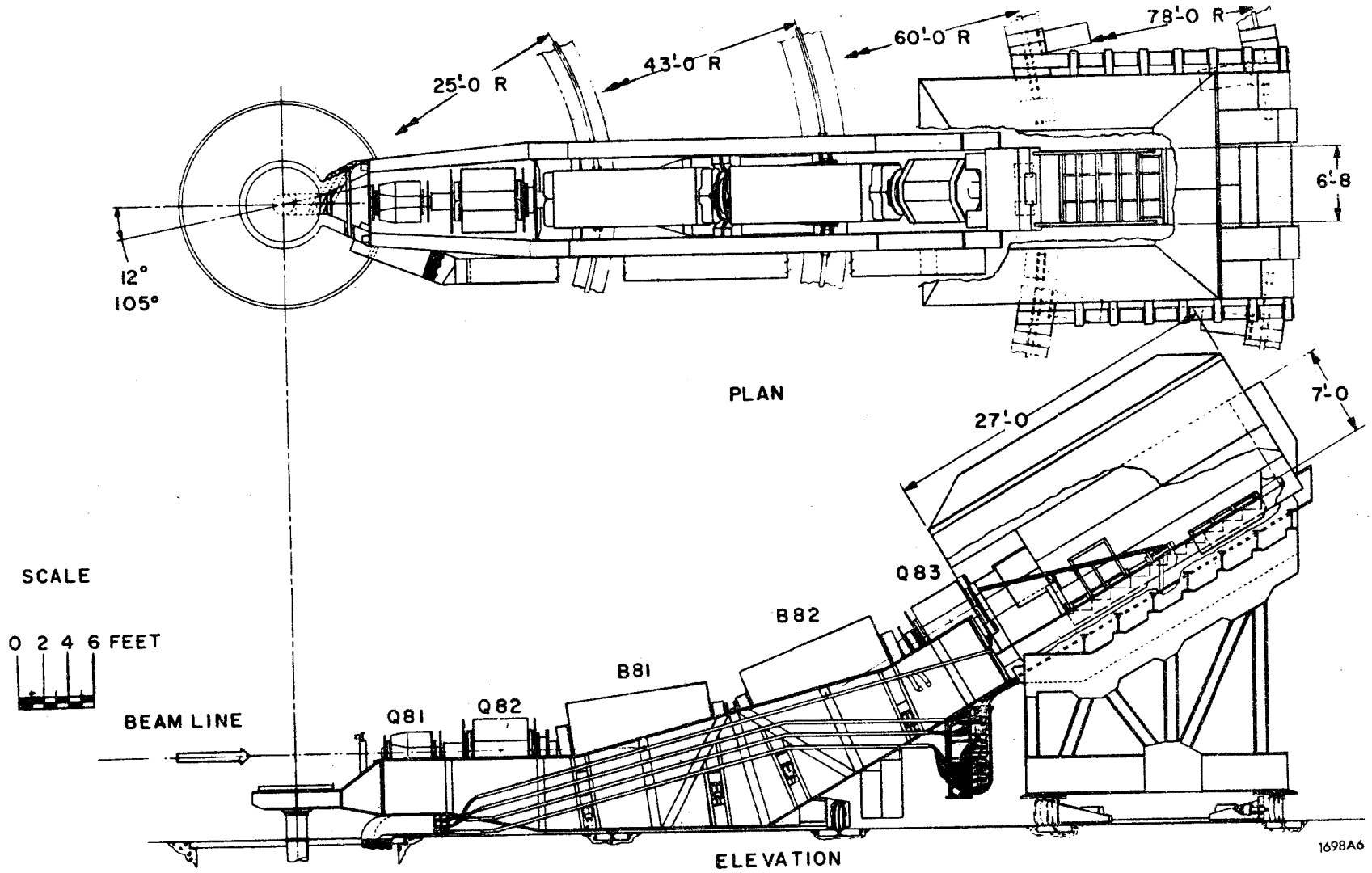
25'-0 R
43'-0 R
60'-0 R
78'-0 R
6'-8
12°
105°
PLAN
7'-0
27'-0
SCALE
0 2 4 6 FEET
Q83
B82
B81
Q82
Q81
BEAM LINE
ELEVATION
1698A6

Fig. 4

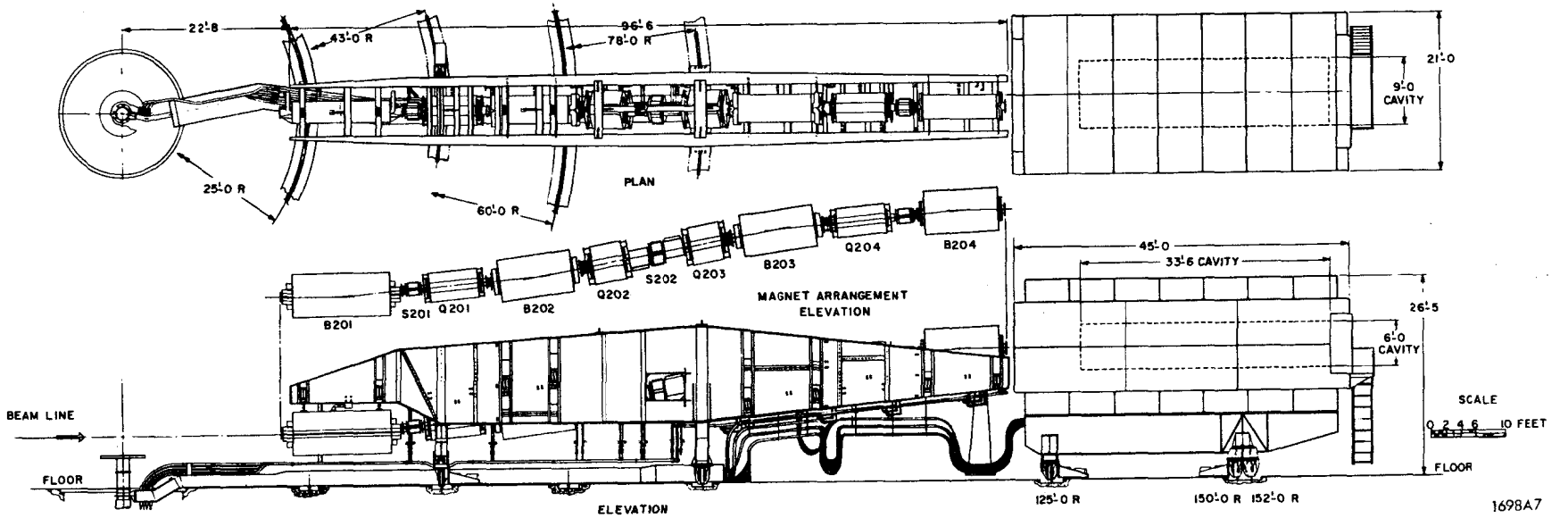
22'-8
43'-0 R
96'-6
78'-0 R
25'-0 R
60'-0 R
PLAN
21'-0
9'-0 CAVITY
B201
S201
Q201
B202
Q202
S202
Q203
B203
Q204
B204
MAGNET ARRANGEMENT
ELEVATION
45'-0
33'-6 CAVITY
26'-5
6'-0 CAVITY
BEAM LINE
FLOOR
ELEVATION
125'-0 R
150'-0 R
152'-0 R
SCALE
0 2 4 6 10 FEET
FLOOR
1698A7

Fig. 5

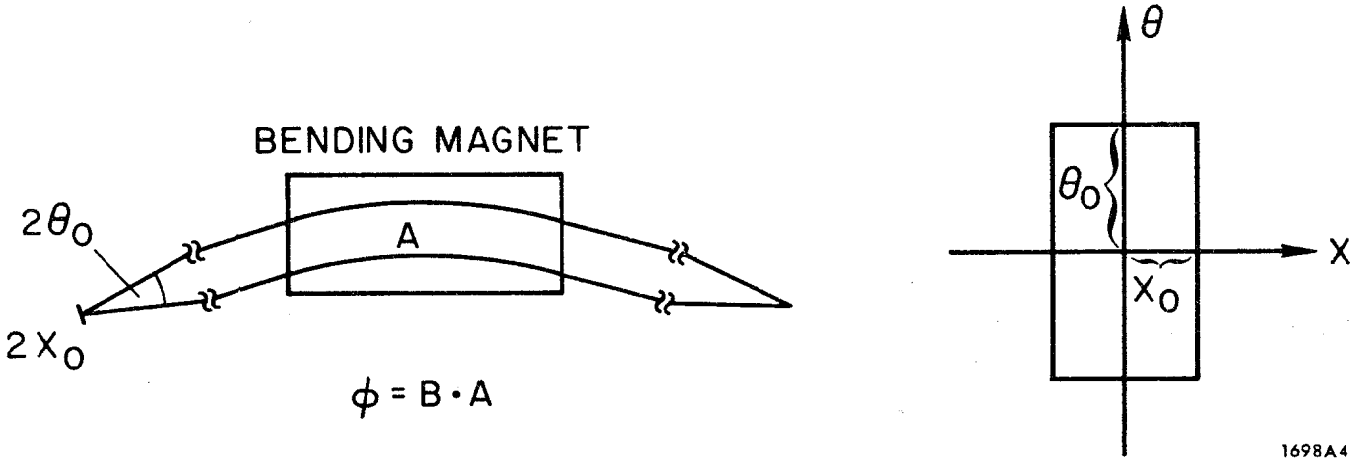

Fig. 6

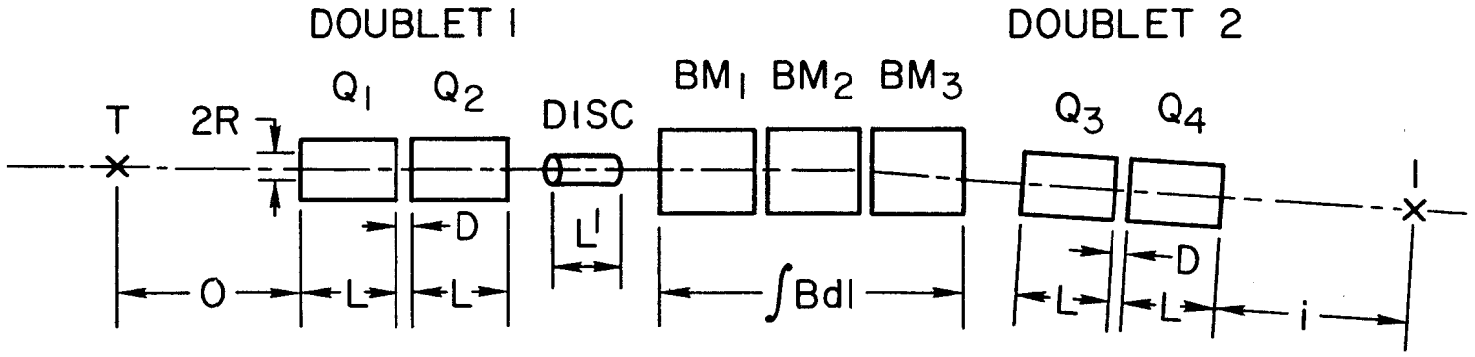

SPECTROMETER OPTICS

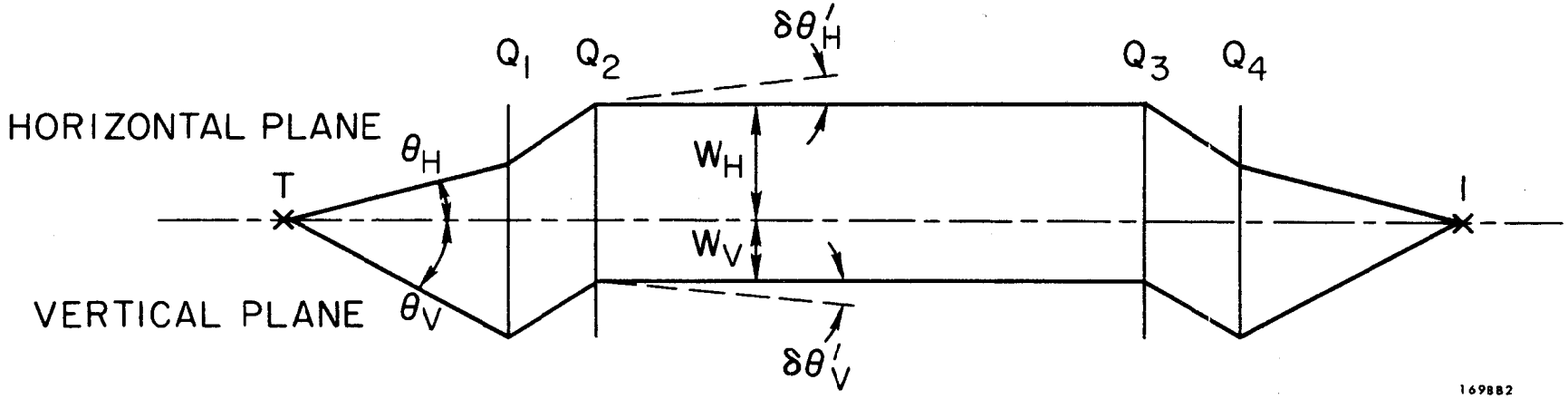

Fig. 7

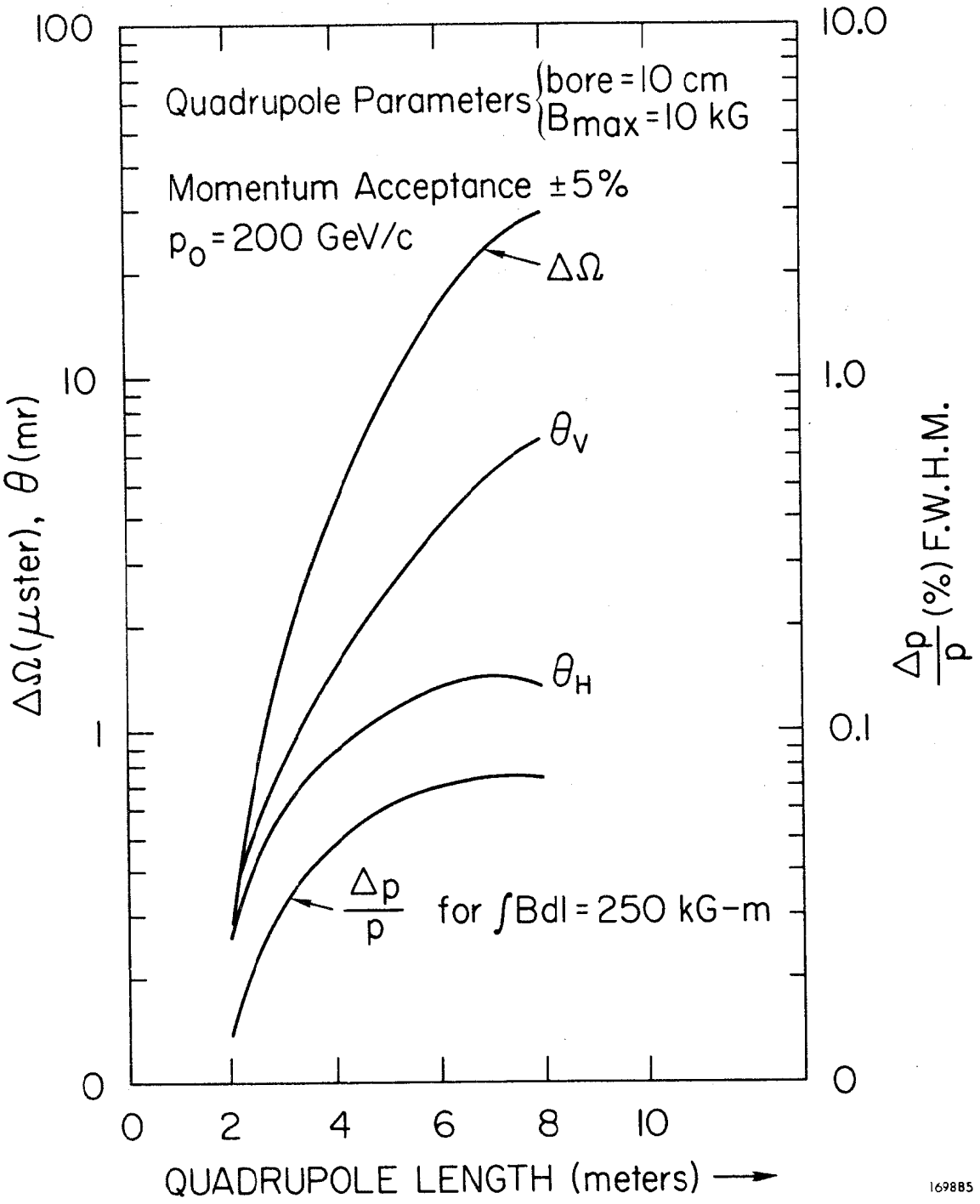
100
10
1
0
10.0
1.0
0.1
0
Quadrupole Parameters
bore = 10 cm
Bmax = 10 kG
Momentum Acceptance ±5%
p0 = 200 GeV/c
ΔΩ
θV
θH
Δp/p
for ∫Bdl = 250 kG-m
0
2
4
6
8
10
QUADRUPOLE LENGTH (meters) →
ΔΩ(μster), θ(mr)
Δp/p (%) F.W.H.M.
169885

Fig. 8

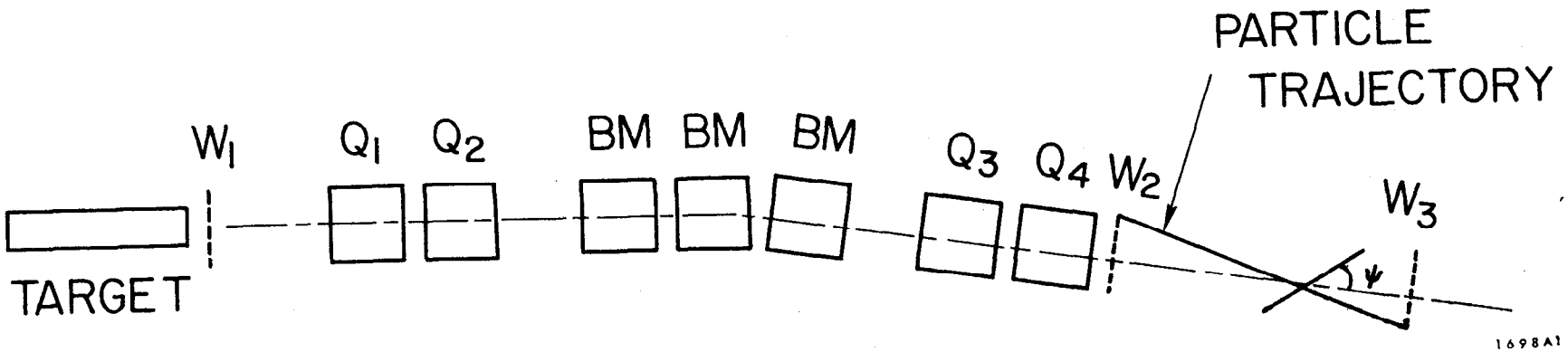
PARTICLE
TRAJECTORY
W1
Q1
Q2
BM
BM
BM
Q3
Q4
W2
W3
TARGET
1698A1

Fig. 9

EFFICIENCY vs MASS SPECTRA

APERTURES I(1.0×0.4m) II(1.8×0.6m) III(2.7×1.8m)

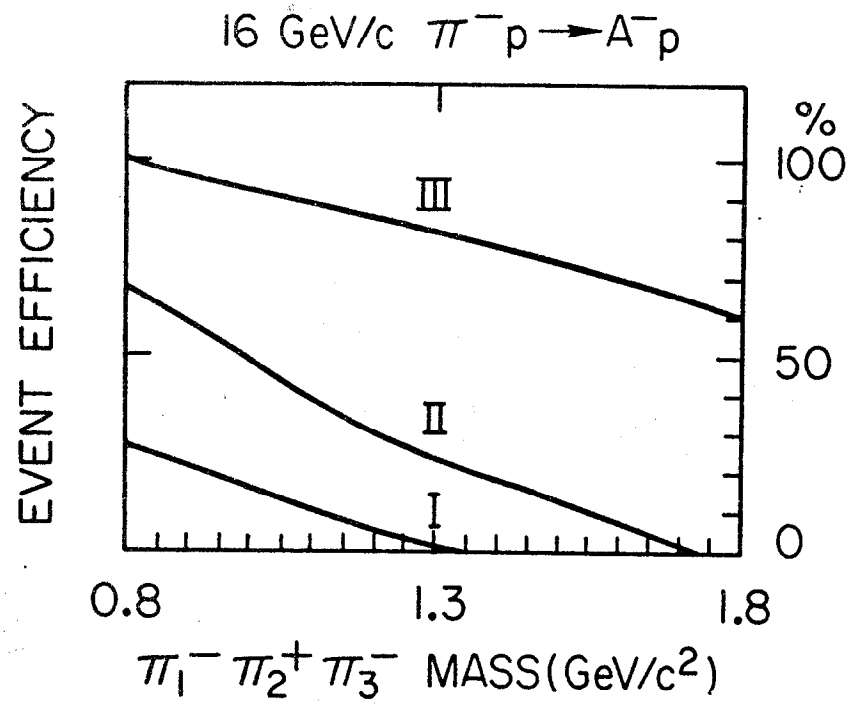

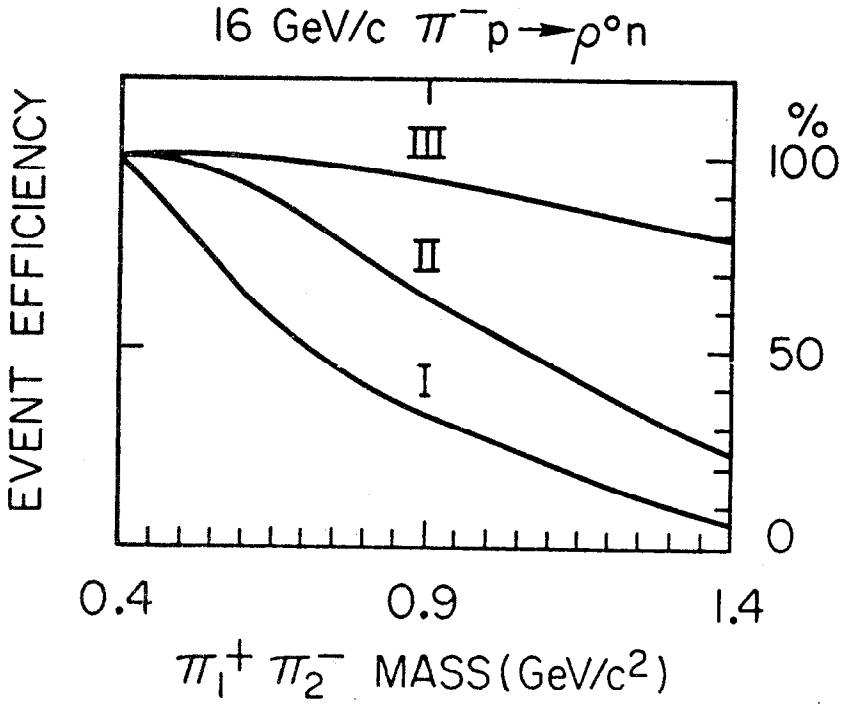

168882

Fig. 10

EFFICIENCY vs DECAY ANGLES
FOR $\rho^0 \rightarrow \pi^+ \pi^-$ IN HELICITY FRAME

APERTURES I(1.0×0.4m) II(1.8×0.6m) III(2.7×1.8m)

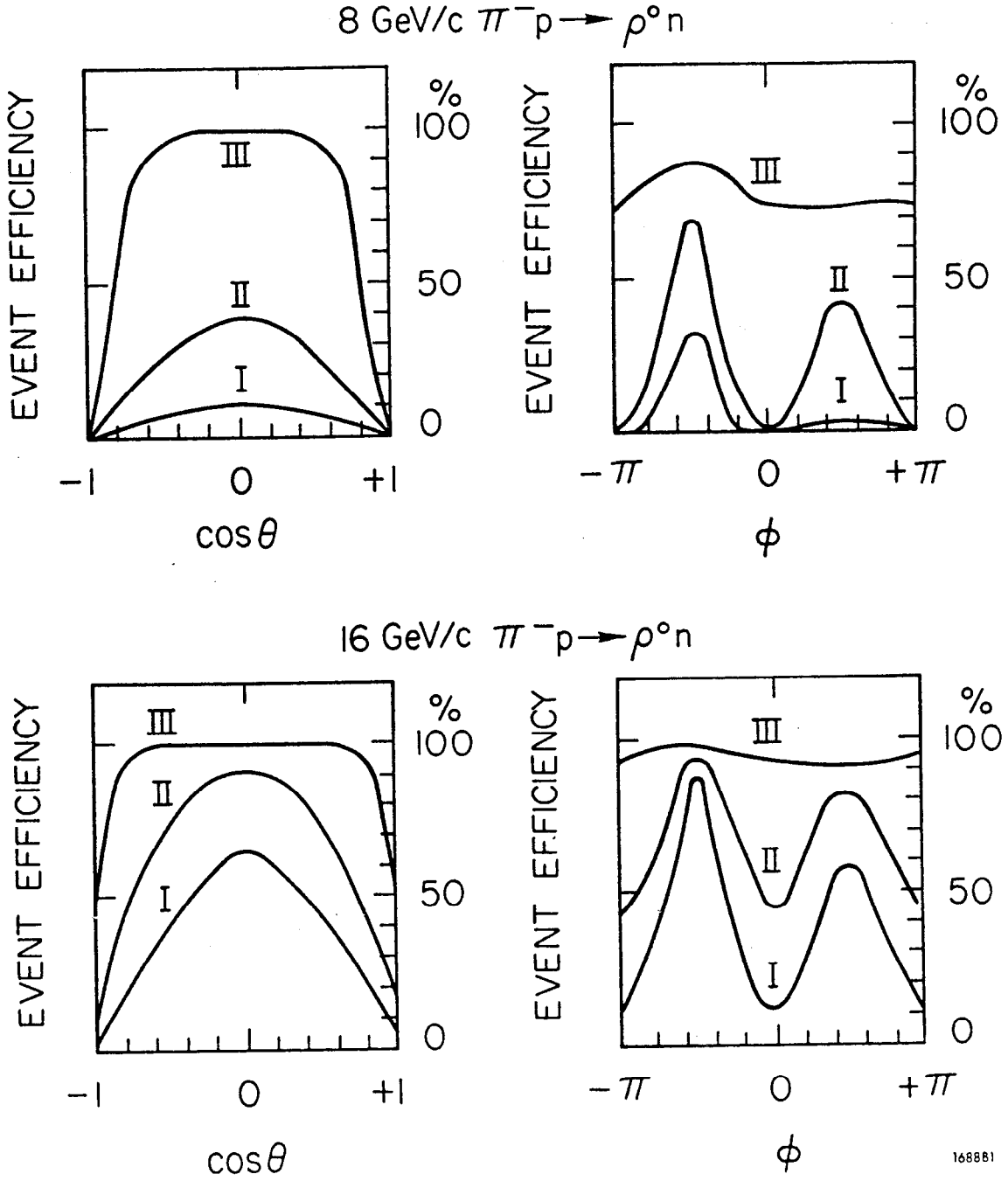

Fig. 11

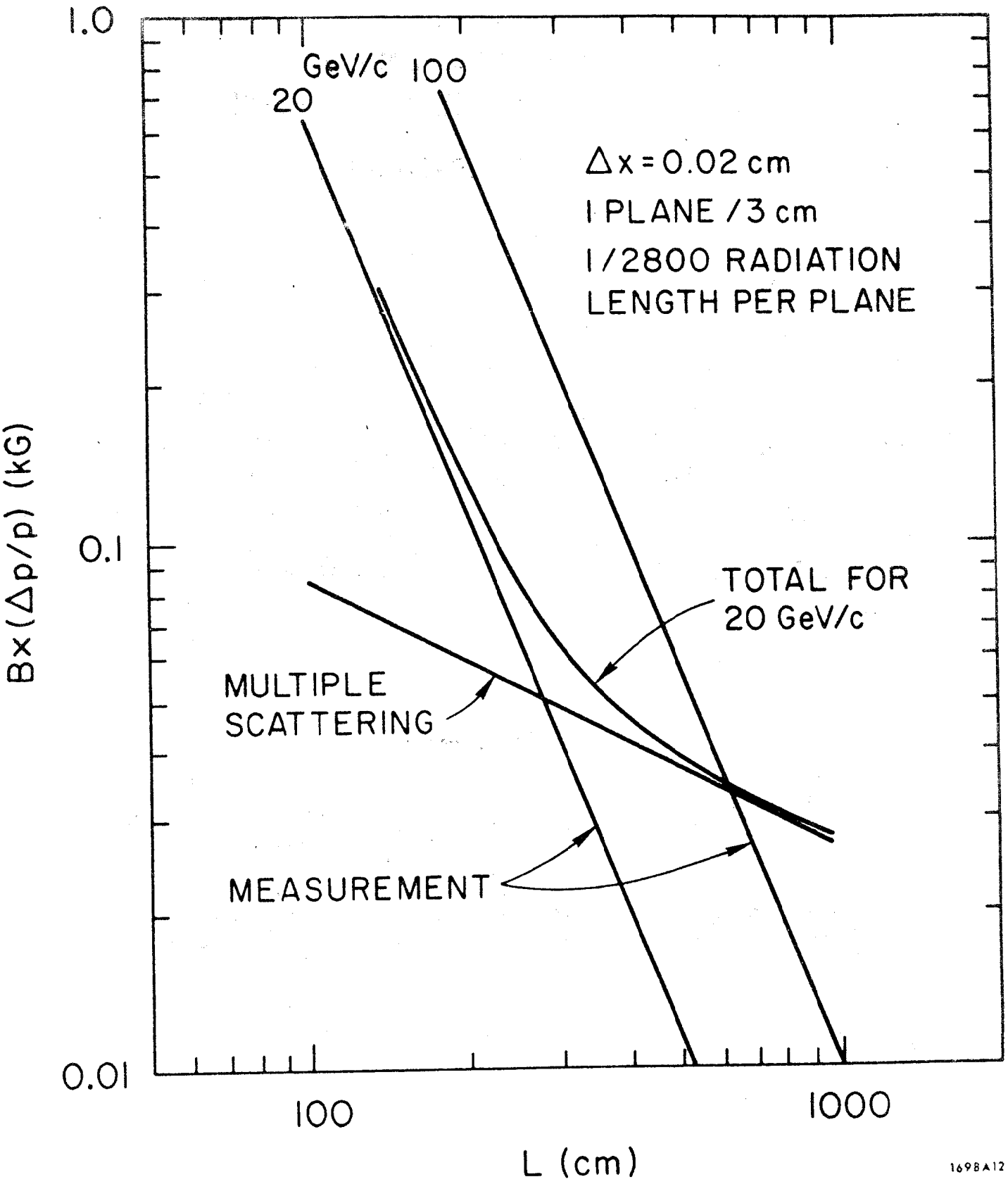
1.0
0.1
0.01
GeV/c
20
100
Δx = 0.02 cm
1 PLANE / 3 cm
1/2800 RADIATION
LENGTH PER PLANE
TOTAL FOR
20 GeV/c
MULTIPLE
SCATTERING
MEASUREMENT
Bx(Δp/p) (kG)
100
1000
L (cm)
1698A12

Fig. 12

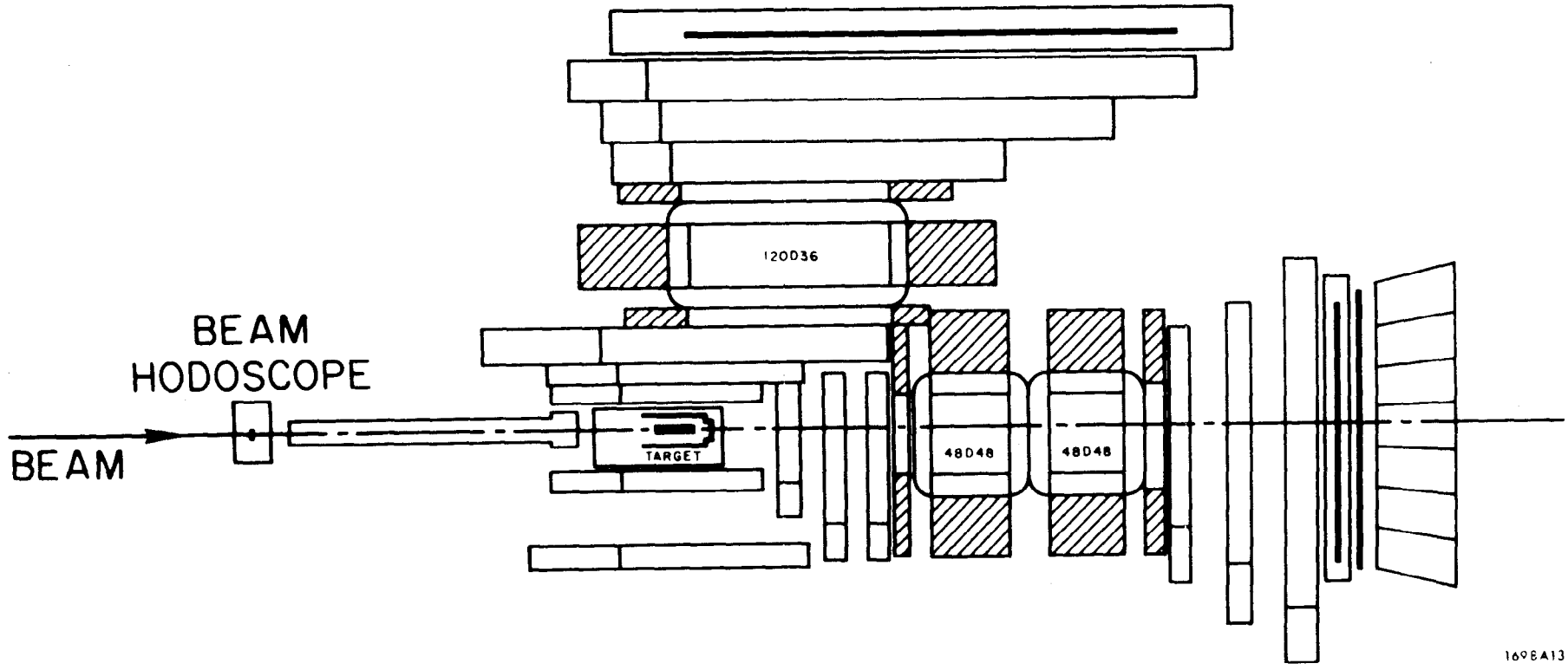

Fig. 13

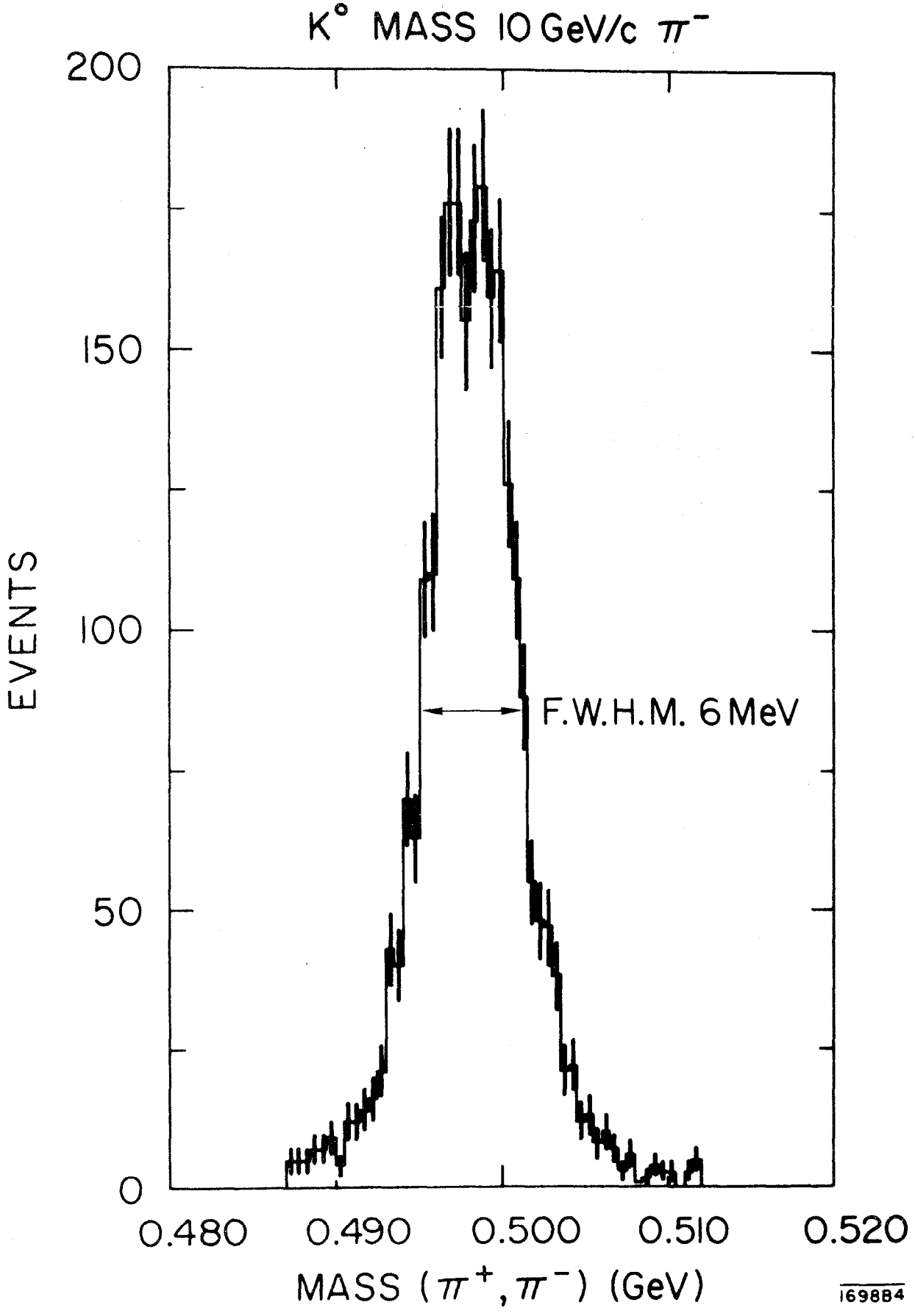
K° MASS 10 GeV/c π⁻
200
150
100
50
0
EVENTS
F.W.H.M. 6 MeV
0.480
0.490
0.500
0.510
0.520
MASS (π⁺, π⁻) (GeV)
169884

Fig. 14

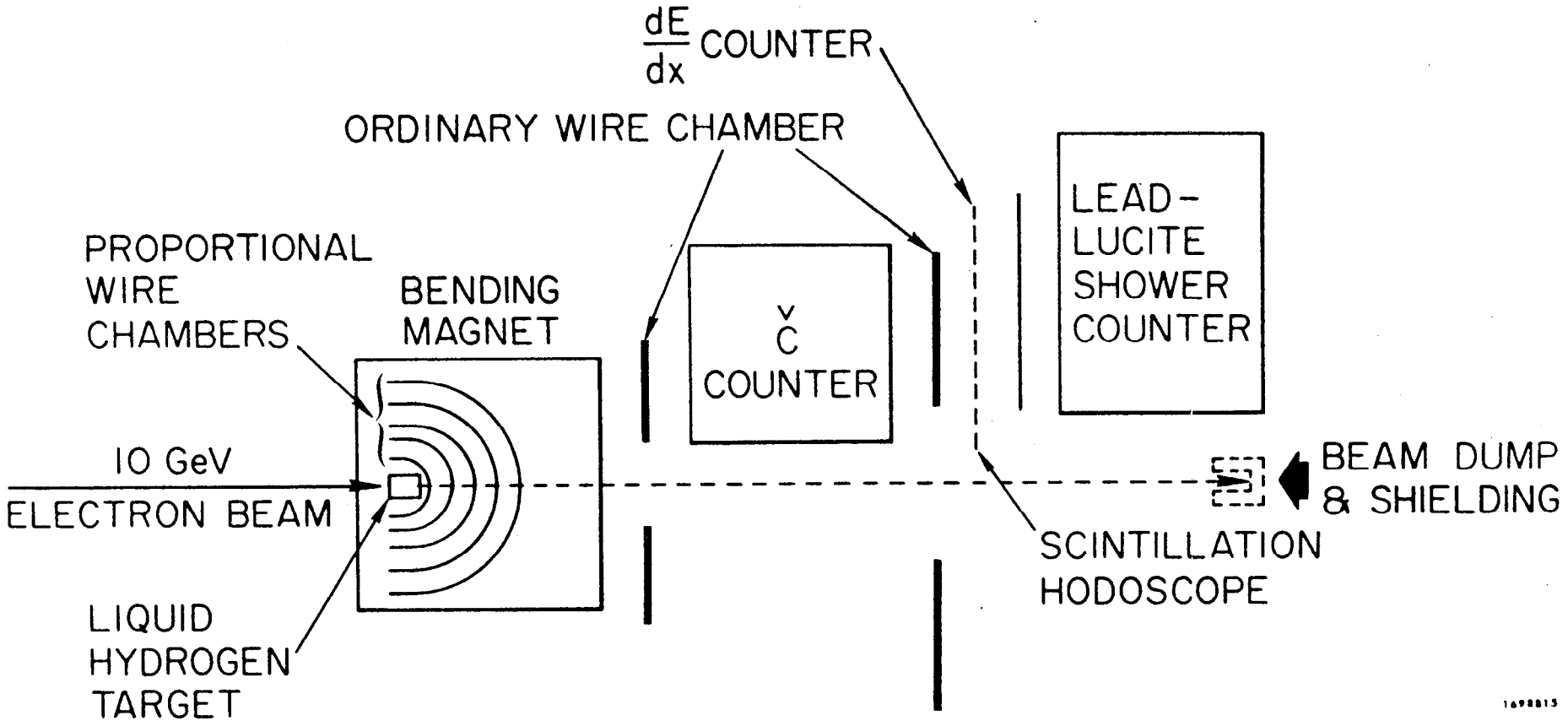
dE/dx COUNTER
ORDINARY WIRE CHAMBER
LEAD-
LUCITE
SHOWER
COUNTER
PROPORTIONAL
WIRE
CHAMBERS
BENDING
MAGNET
v
C
COUNTER
10 GeV
ELECTRON BEAM
BEAM DUMP
& SHIELDING
SCINTILLATION
HODOSCOPE
LIQUID
HYDROGEN
TARGET

Fig. 15

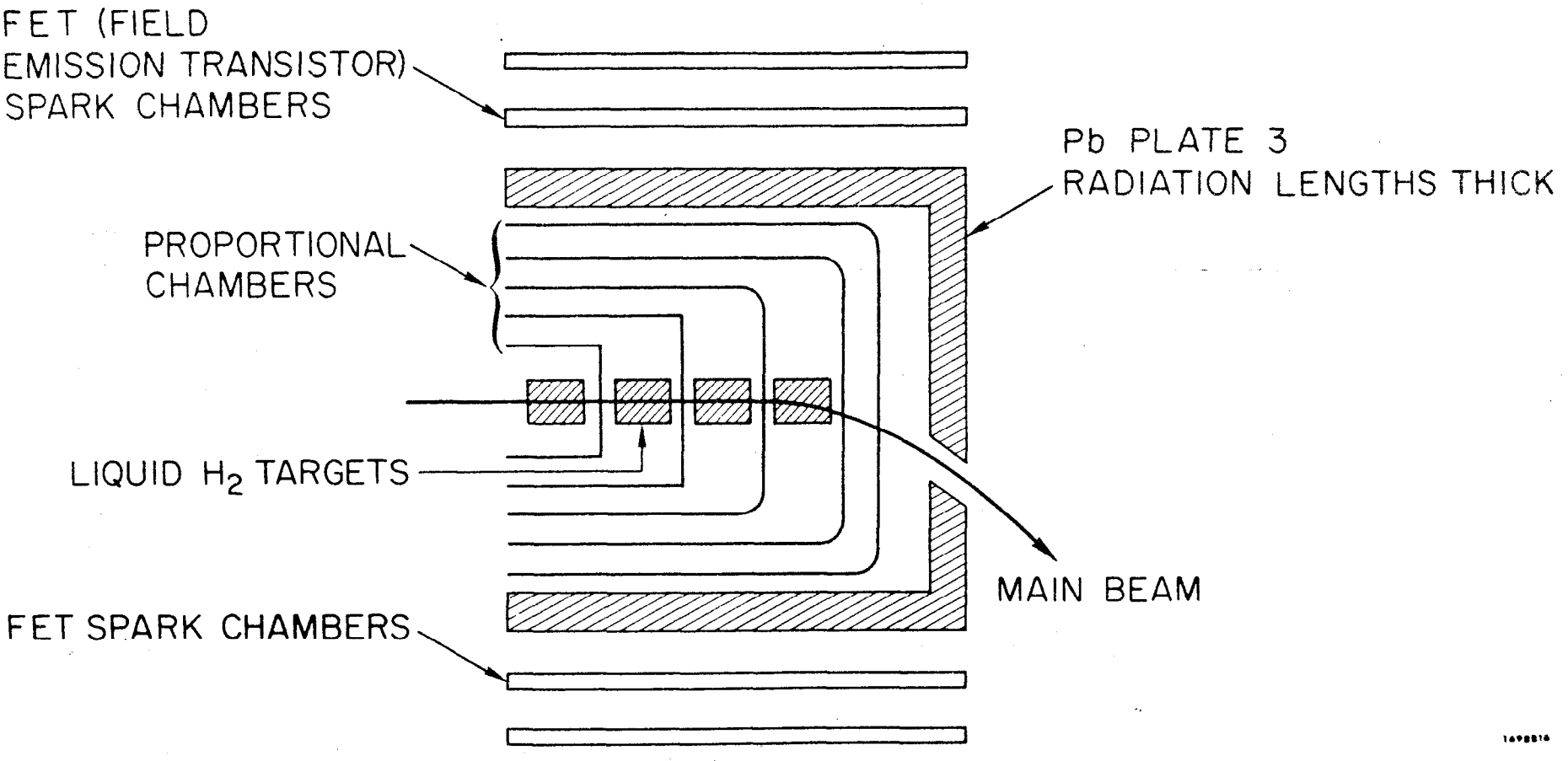
FET (FIELD
EMISSION TRANSISTOR)
SPARK CHAMBERS
Pb PLATE 3
RADIATION LENGTHS THICK
PROPORTIONAL
CHAMBERS
LIQUID H_2 TARGETS
MAIN BEAM
FET SPARK CHAMBERS

Fig. 16

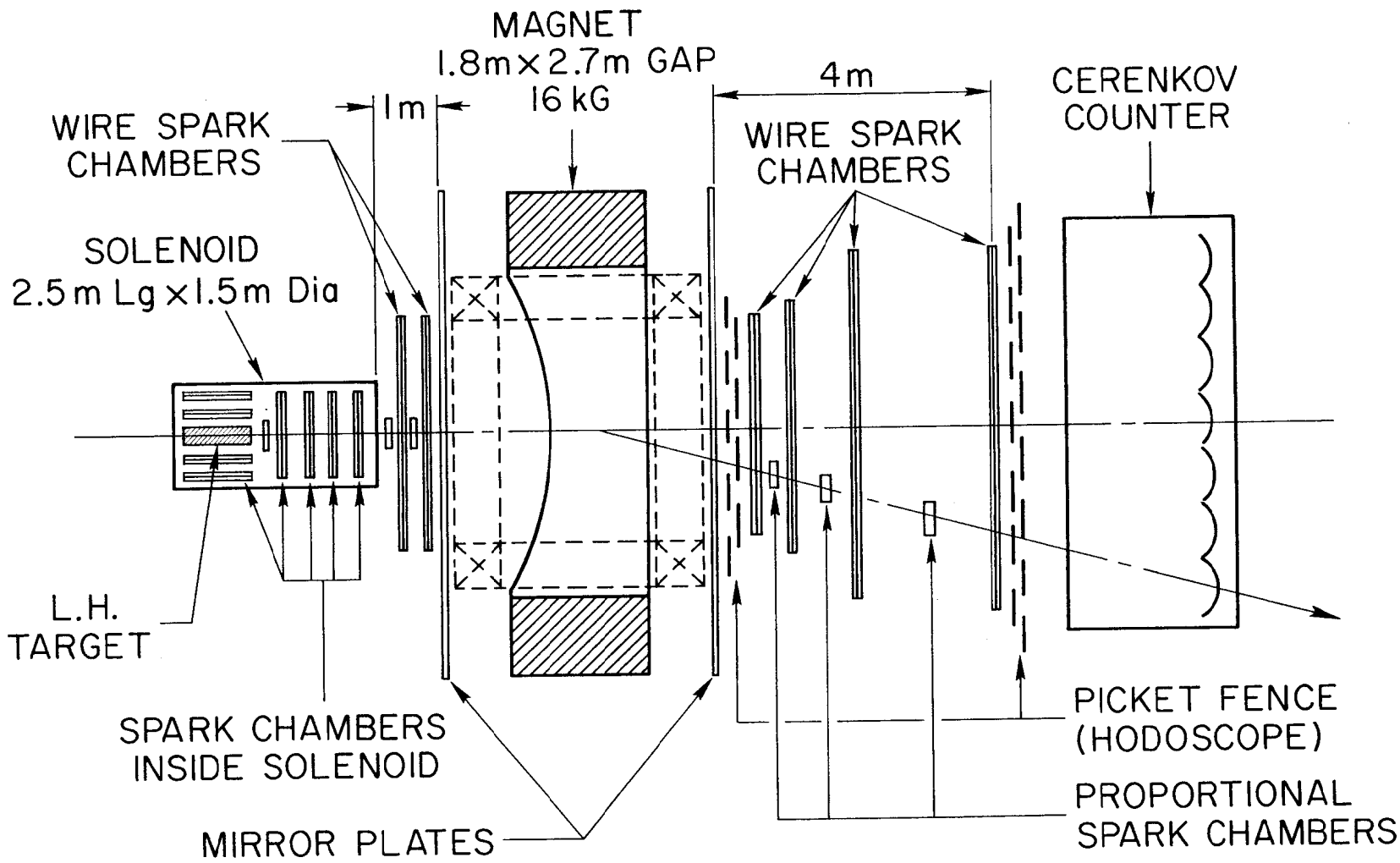

SLAC LARGE WIRE SPARK CHAMBER

1611A2

Fig. 17

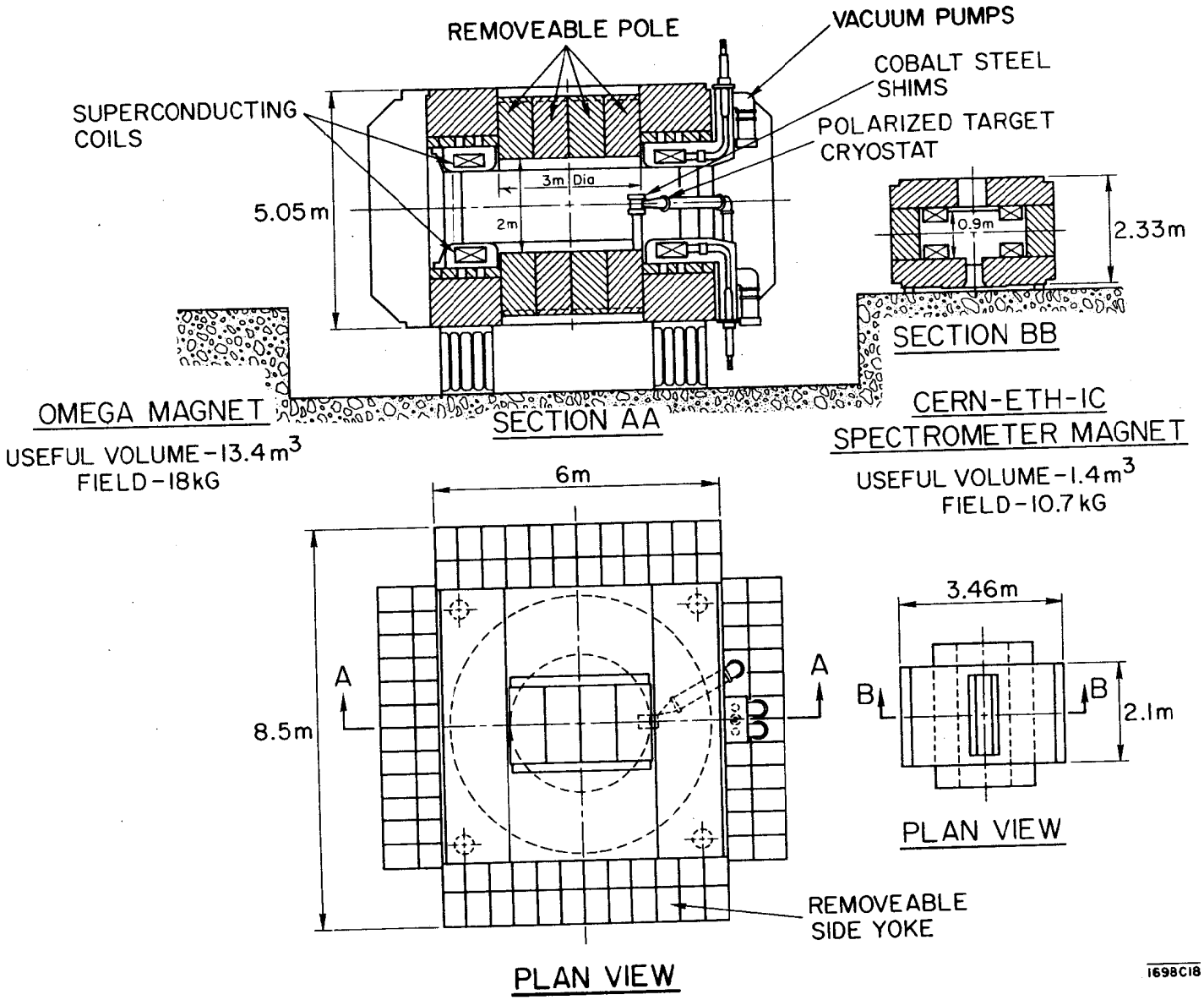
REMOVEABLE POLE
VACUUM PUMPS
COBALT STEEL SHIMS
POLARIZED TARGET CRYOSTAT
SUPERCONDUCTING COILS
3m Dia
2m
5.05m
0.9m
2.33m
SECTION BB
SECTION AA
OMEGA MAGNET
USEFUL VOLUME-13.4m3
FIELD-18kG
CERN-ETH-IC
SPECTROMETER MAGNET
USEFUL VOLUME-1.4m3
FIELD-10.7kG
6m
A
A
8.5m
3.46m
B
B
2.1m
PLAN VIEW
REMOVEABLE SIDE YOKE
PLAN VIEW
1698C18

Fig. 18